ACS APPLIED MATERIALS & INTERFACES

Letter

www.acsami.org

Self-Assembled Poly(3,4-ethylene dioxythiophene):Poly(styrenesulfonate)/Graphene Quantum Dot Organogels for Efficient Charge Transport in Photovoltaic Devices

Hong Chul Lim,[†,‡] Sa Hoon Min,[†,§] Eunwoo Lee,[⊥] Jyongsik Jang,[⊥] Sung Hyun Kim,*[,‡] and Jong-In Hong*[,‡]

[‡]Department of Chemistry, and [⊥]World Class University (WCU) Program of Chemical Convergence for Energy and Environment (C2E2), School of Chemical and Biological Engineering, College of Engineering, Seoul National University, Seoul 151-747, Republic of Korea

[§]Department of Energy Engineering, School of Energy and Chemical Engineering, Ulsan National Institute of Science and Technology (UNIST), Ulsan 689-798, Korea

Supporting Information

ABSTRACT: We report the self-assembly of poly(3,4-ethylene dioxythiophene):poly(styrenesulfonate) (PEDOT:PSS) organogel films incorporating graphene quantum dots (GQDs). Because of the electrostatic interaction between the GQDs and the PEDOT chains, GQD@PEDOT core−shell nanostructures are readily formed. We demonstrate that the GQDs affect the reorientation of PEDOT chains and the formation of interconnected structure of PEDOT-rich domains, improving the charge transport pathway. The power conversion efficiency of the organic photovoltaic device containing the self-assembled organogel as the hole extraction layer (HEL) was 26% higher than the device with pristine PEDOT−PSS as the HEL.

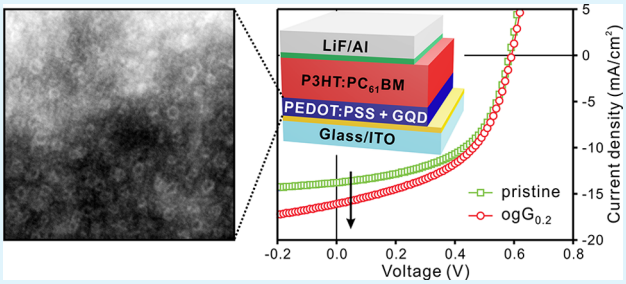

KEYWORDS: *self-assembly, organogel, PEDOT:PSS, graphene quantum dots, organic photovoltaics*

Organic photovoltaics (OPVs) have drawn much attention as potential next-generation renewable energy sources on account of low production costs and solution processability, which make mass production of OPVs viable.[1−4] To fabricate OPVs, we inserted poly(3,4-ethylenedioxythiophene):poly(styrenesulfonate) (PEDOT:PSS) as the hole extraction layer (HEL) between the anode and the active layer to overcome issues arising from energy level alignment and the surface roughness of anode.[5−8] However, PEDOT:PSS shows poor electrical properties because the PSS chains, which are the counterions of PEDOT, are insulators. The electrical properties of PEDOT:PSS are usually improved by solvent or acid treatment,[9−13] annealing,[14,15] and by adding organic compounds[16−18] affecting the orientation of the PEDOT chains within the matrix, leading to expanded-coil conformation that strengthen interactions between the PEDOT chains. These strategies focus on increasing the conductivity of PEDOT:PSS by controlling the PEDOT chain orientation, but unfortunately the improvement of OPV performance was not directly proportional to the increase in conductivity. Thus, fine-tuning the orientation and morphology of PEDOT:PSS to improve electrical percolation pathways for achieving optimized device efficiency remains a challenge.

Recently, graphene oxide (GO), a two-dimensional carbon allotrope, has been used to improve the electrical properties of PEDOT:PSS by gelation,[19−21] although GO by itself is insulating. These studies indicate that GO can also act as an effective additive for PEDOT:PSS; however, the aggregation of large-sized GO sheets and their wide size distribution make it difficult to achieve the fine-tuning of the electrical properties of PEDOT:PSS for practical applications. In this letter, we report the synthesis of PEDOT:PSS organogels incorporating relatively uniform-sized graphene quantum dots (GQDs). The GQDs can act as a physical linker among PEDOT chains through electrostatic interaction, resulting in the formation of core−shell nanostructure. The nanoscopic morphology and orientation of PEDOT:PSS in the organogel were investigated to clarify the influence of the incorporation of GQD on their electrical properties. The PEDOT:PSS films containing the GQDs were subsequently used as the HEL in a typical poly(3-hexylthiophene) (P3HT):[6,6]-phenyl-C_{61}-butyric acid methyl ester (PCBM) bulk heterojunction OPV.

The pristine GQDs were fabricated from carbon nanofibers (CNFs) via excess oxidation and size-selective precipitation. The as-synthesized GQDs with a diameter of about 8−10 nm were characterized by high-resolution transmission electron

Received: March 19, 2015
Accepted: May 18, 2015
Published: May 18, 2015

DOI: 10.1021/acsami.5b02434
ACS Appl. Mater. Interfaces 2015, 7, 11069−11073

microscopy (HRTEM) (Figure 1a). The results are consistent with structures previously reported.[22] The organogel was

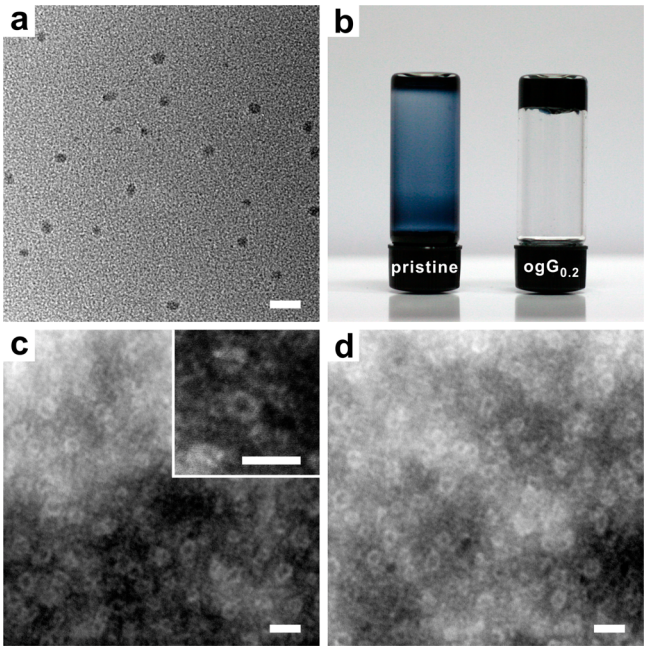

Figure 1. (a) High-resolution transmission electron microscopy (HRTEM) image of the as-synthesized GQDs. (b) Photograph of the pristine PEDOT:PSS and the self-assembled organogel. Cross-sectional high-angle annular dark-field scanning TEM (HAADF-STEM) images of (c) $ogG_{0.2}$ and (d) $ogG_{0.5}$ PEDOT:PSS organogel with 20 vol % and 50 vol % GQD solution, respectively. The inset shows the magnified the core−shell nanostructures (CSNSs). All the scale bars are 20 nm.

prepared by mixing a GQD (0.19 wt %)-isopropyl alcohol (IPA) solution with a 70 vol % aqueous solution of PEDOT:PSS (CLEVIOS PH500) in IPA. The mixture was left undisturbed for 1 h. Consequently, the PEDOT:PSS solution readily formed viscous organogels, as shown in Figure 1b. The prepared organogels are termed as $ogG_{0.2}$ and $ogG_{0.5}$ with the subscripts denoting the volume fraction of the GQD solution. As a control, pristine PEDOT:PSS sample was also treated with IPA and prepared with the same procedure without GQDs. Figure 1c, d shows the cross-sectional high-angle annular dark-field scanning TEM (HAADF-STEM) image of the organogel films obtained by drying the solvent. Interestingly, the results indicate the formation of core−shell nanostructure (CSNS) with an average diameter of about 12 nm in the organogel, whereas the pristine PEDOT:PSS only had a granular structure of the PEDOT:PSS agglomeration in the matrix.[12,23] Because of the high GQD content in PEDOT:PSS, $ogG_{0.5}$ showed more aggregated CSNSs than $ogG_{0.2}$, although their morphologies were similar. It is noteworthy that the core size of the CSNSs is almost identical to the as-synthesized GQD diameter. Because the HAADF-STEM image of as-synthesized GQD only shows a particlelike structure (Figure S1 in the Supporting Information) and the brightness of the HAADF-STEM image is proportional to the sample thickness and the square of the atomic number,[23] it is obvious that the bright shell (ca. 2.5 nm in thickness) in the HAADF-STEM images indicates the agglomeration of PEDOT:PSS chains on the GQD.

To clarify the PEDOT:PSS agglomeration, we acquired X-ray diffraction (XRD) patterns of PEDOT:PSS films obtained with various volume fractions of GQD solutions, as shown in Figure 2a. The pristine PEDOT:PSS film exhibited two broad peaks at

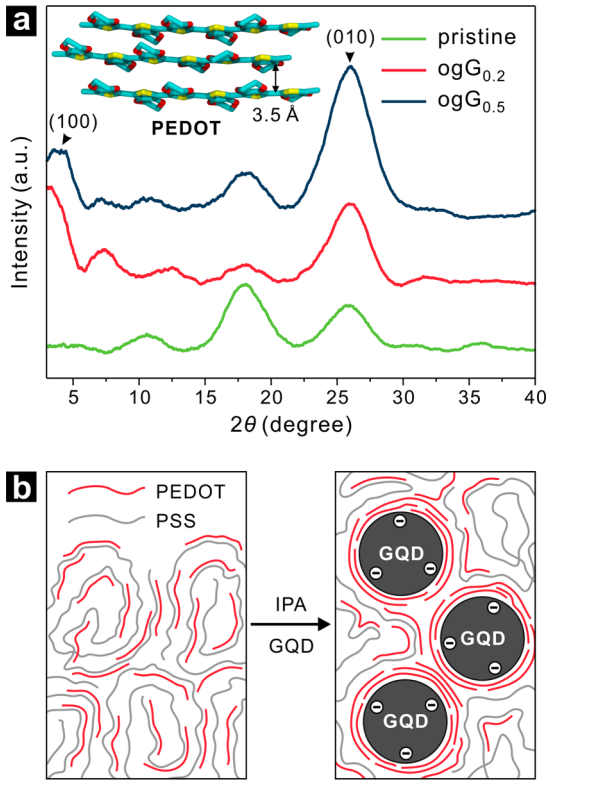

Figure 2. (a) X-ray diffraction (XRD) patterns of the PEDOT:PSS organogel films obtained with volume fractions of GQD solution. The inset shows the molecular structure of crystalline PEDOT chains with the (010) lattice spacing. (b) Schematic representation of the formation of the GQD@PEDOT CSNS.

2θ = 25.8 and 18.0°, which correspond to the $\pi-\pi$ interchain stacking of PEDOT and the amorphous halos of PSS chains, respectively.[12,24] In the case of the organogel with GQDs, the XRD patterns indicate a significant increase in the peak intensity at 2θ = 3.5 and 25.8°, representing the enhancement of the crystalline structure along the (100) and (010) lattices, corresponding to the lamella stacking and interchain stacking of PEDOT chains, respectively.[25] With increase in the GQD solution volume fraction, the crystallinity of the PEDOT interchain stacking (d-spacing = 3.5 Å) gradually increased; however, the crystallinity corresponding to the lamella stacking of PEDOT showed no significant difference in terms of the peak intensity. Notably, the peak intensity at 2θ = 18.0°, corresponding to the interchain stacking of PSS chains reduced after the addition of GQDs. The intensity ratio of the peaks at 2θ = 25.8 and 18.0° (i.e., the ratio of the interchain stacking of PEDOT to PSS) was about four times larger than that shown by samples without GQDs. From these results, the agglomeration of PEDOT:PSS chains onto the GQDs might mainly lead to ordered crystalline PEDOT with interchain $\pi-\pi$ stacking. Thus, the bright shell in the HAADF-STEM images indicates the agglomeration of the stacked PEDOT chains on the surface of the GQDs.

We propose a model to explain the formation of the GQD@PEDOT CSNS shown in Figure 2b. It is known that the

DOI: 10.1021/acsami.5b02434
ACS Appl. Mater. Interfaces 2015, 7, 11069−11073

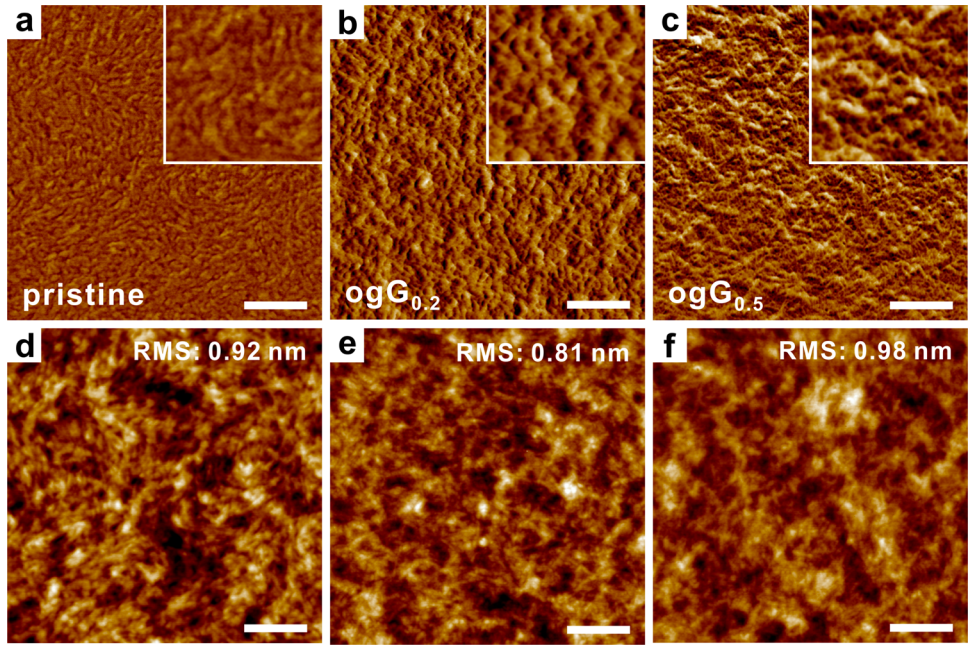

Figure 3. Phase and topographic images of PEDOT:PSS organogel films of (a, d) pristine PEDOT:PSS, (b, e) $ogG_{0.2}$, and (c, f) $ogG_{0.5}$ samples. All scale bars are 200 nm.

insulating PSS counterions enable the conducting PEDOT chains to exist as a stable aqueous suspension through Coulomb interaction. The addition of IPA into the PEDOT:PSS aqueous solution readily weakens the Coulomb interaction between the positively charged PEDOT and negatively charged PSS components by the screening effect, resulting in a conformational transition into an extended-coil structure of PEDOT.[26] Subsequently, the addition of GQDs would allow the extended PEDOT chains to interact with the GQDs because of the presence of abundant negatively charged functional groups on the GQD surface. During gelation, the PEDOT chains preferentially interacting with the GQDs were stacked on the GQD surface because of the electrostatic interaction as well as $\pi-\pi$ stacking,[13] leading to the formation of CSNSs.

The addition of GQDs affected the surface morphology of the PEDOT:PSS film as well as the interactions between the PEDOT chains in the polymer matrix. Figure 3 shows the nanoscopic morphology of the PEDOT:PSS film with GQDs obtained by atomic force microscopy (AFM). The phase image of the pristine PEDOT:PSS demonstrated phase separation between them where each domain had a disconnected and isolated nanostructure (Figure 3a) with the bright and dark regions in the phase image of PEDOT:PSS representing the PEDOT-rich and PSS-rich domains, respectively.[11] In contrast, Figure 3b, c, which are images from samples containing the GQDs, show relatively homogeneous and interconnected PEDOT-rich domains. This morphological transition of the PEDOT-rich domain implies that the GQDs not only act as physical linkers within the organogels, but also hold the PEDOT-rich domains by the aggregation of CSNSs. The topological images of the organogels also reveal a more interconnected and reticulated structure. The formation of the reticulated structure was observed by a time-dependent AFM study during the gelation, as shown in Figure S2 (Supporting Information). Interestingly, the incorporation of GQD did not significantly affect the surface roughness of PEDOT:PSS film in contrast with the incorporation of GO sheets,[21] because of the small-sized GQD. In addition, the organogel films also showed a high transparency (Figure S3 in the Supporting Information), similar to the PEDOT:PSS/GO composite.[19]

The reorientation of PEDOT chains with phase separation is advantageous in enhancing the conductivity of PEDOT:PSS because of the lowered energy barrier required for charge hopping across the domains and chains.[11] Because the PEDOT chains in the organogel prefer to interact with each other in the CSNS and the PEDOT-rich domains show a three-dimensionally interconnected structure in the PEDOT:PSS matrix simultaneously, the charge hopping pathway is improved, leading to enhanced conductivity of the organogel.

The organogel films were used as the HEL in P3HT/PCBM bulk heterojunction OPVs fabricated by solution-processing (Figure 4a). The characteristic parameters, such as the open-circuit voltage (V_{OC}), short-circuit current (J_{SC}), fill factor (FF), and power conversion efficiency (PCE), are summarized in Table 1. Because the work function of the GQD film was 5.0 eV (as obtained by ultraviolet photoelectron spectroscopy), the energy barrier to hole injection between the anode and the HEL was insignificantly affected by the GQD incorporation. Minor differences were also identified in V_{OC} among the OPVs, indicating that the ohmic contact of the anode/active layer was maintained in the presence of GQDs. These results suggest that including GQDs in the HEL preserves the interfaces of the OPV system without disruption.

Indeed, using $ogG_{0.2}$ as the HEL leads to an increase in the PCE by 26% compared to the PCE of the OPV with pristine PEDOT:PSS as the HEL. This significant enhancement in PCE is mainly attributed to the increase in J_{SC}, resulting from the enhanced conductivity and lowered series resistance of the organogel, as shown in Figure 4b. The organogels showed more than four times higher conductivity in comparison to the pristine PEDOT:PSS whose conductivity was just about 1 S/cm. It can support the fact that the CSNSs provide a better pathway for the charge hopping with three-dimensionally

DOI: 10.1021/acsami.5b02434
ACS Appl. Mater. Interfaces 2015, 7, 11069−11073

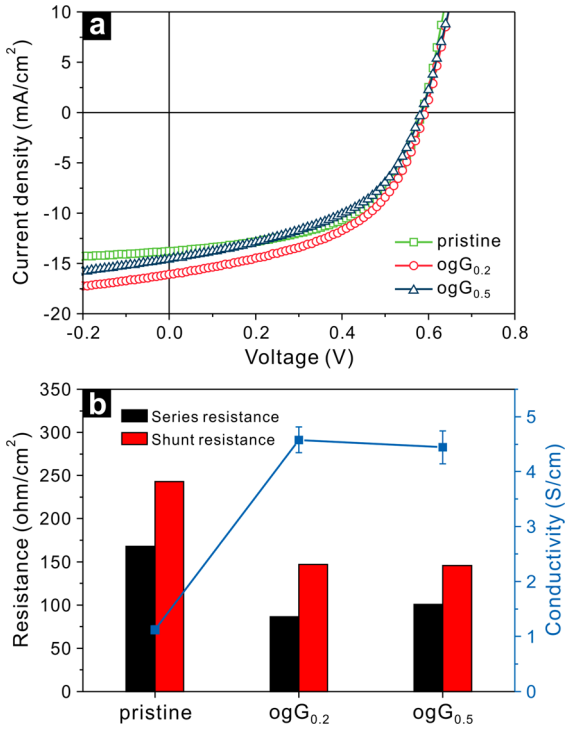

Figure 4. (a) Current density–voltage (J–V) characteristics of the OPV with the pristine PEDOT:PSS, ogG$_{0.2}$, and ogG$_{0.5}$ as the hole extraction layer (HEL). (b) Series and shunt resistances of OPVs and the conductivity of the pristine PEDOT:PSS, ogG$_{0.2}$, and ogG$_{0.5}$ films.

Table 1. Photovoltaic Performance of OPVs with Various HELs[a]

HEL	J_{SC} (mA cm^{-2})	V_{OC} (V)	FF	PCE (%)
pristine	11.97	0.58	0.54	3.77
ogG$_{0.2}$	16.08	0.59	0.50	4.74
ogG$_{0.5}$	14.59	0.58	0.48	4.08

[a]Device structure in all cases is ITO/HEL/P3HT:PC$_{61}$BM/LiF/Al.

interconnected structure of the HEL. However, the enhanced charge hopping pathway in the HELs with the GQDs shows a negative effect on FF. In general, the decrease in FF is related to the increase in series resistance or the decrease in shunt resistance of OPV.[27] The shunt resistance is also reduced with the incorporation of the GQDs, resulting in a leakage current between the electrodes. In contrast, the OPV with ogG$_{0.5}$ as the HEL showed a decrease in both J_{SC} and FF, and a small increase in device efficiency. The increased series resistance of ogG$_{0.5}$ in comparison to that of ogG$_{0.2}$ implies that excess GQDs disrupt charge transport within the HEL because of the aggregation of CSNSs and the higher population of the insulating GQDs. Thus, ogG$_{0.2}$ is considered as the optimum HEL to yield OPVs with the best performance.

In conclusion, we have successfully demonstrated a simple process to fabricate a PEDOT:PSS-based organogel containing GQDs for efficient charge transport in a HEL of OPVs. The organogel film consisted of PEDOT-rich domains in the matrix, formed by stacking PEDOT chains on the surface of GQDs, leading to CSNSs. These structures were formed because of the electrostatic interactions between the components. Furthermore, during gelation, three-dimensionally interconnected structures were also formed in the organogel film through the aggregation of the GQD@PEDOT CSNSs, which improved the charge transport pathway. The use of organogel films with these distinct conformations and morphologies of the PEDOT-rich domains improved the OPV performance by up to 26% (in comparison to that of the OPV containing the pristine PEDOT:PSS as HEL). These results suggest that incorporation of GQDs in the organogel is compatible with the solution processing of OPV devices and is a promising strategy for enhancing the electrical properties of PEDOT:PSS, leading to the performance enhancement in flexible devices such as OPVs and polymer-based light-emitting diodes.

■ ASSOCIATED CONTENT

Supporting Information

Experimental section, HAADF-STEM image of the as-synthesized GQDs, time-dependent AFM images during gelation, and UV/vis transmittance spectra of the organogels. The Supporting Information is available free of charge on the ACS Publications website at DOI: 10.1021/acsami.5b02434.

■ AUTHOR INFORMATION

Corresponding Authors

*E-mail: shkim75@snu.ac.kr.
*E-mail: jihong@snu.ac.kr.

Author Contributions

†H.C.L. and S.H.M. contributed equally to this work.

Notes

The authors declare no competing financial interest.

■ ACKNOWLEDGMENTS

This work was supported by the NRF grant (2013R1A1A2074468) funded by the MSIP, the Industrial Strategic Technology Development Program (10042412) funded by Ministry of Trade, Industry and Energy (MOTIE, Korea), and Basic Science Research Program through the National Research Foundation of Korea (NRF) funded by the Ministry of Education, Science and Technology (2013-024206).

■ REFERENCES

(1) Liu, Z.; Li, J.; Yan, F. Package-Free Flexible Organic Solar Cells with Graphene Top Electrodes. *Adv. Mater.* **2013**, *25*, 4296–4301.

(2) You, J.; Dou, L.; Yoshimura, K.; Kato, T.; Ohya, K.; Moriarty, T.; Emery, K.; Chen, C.-C.; Gao, J.; Li, G.; Yang, Y. A Polymer Tandem Solar Cell with 10.6% Power Conversion Efficiency. *Nat. Commun.* **2013**, *4*, 1446.

(3) Facchetti, A. Π-Conjugated Polymers for Organic Electronics and Photovoltaic Cell Applications. *Chem. Mater.* **2011**, *23*, 733–758.

(4) Günes, S.; Neugebauer, H.; Sariciftci, N. S. Conjugated Polymer-Based Organic Solar Cells. *Chem. Rev.* **2007**, *107*, 1324–1338.

(5) Guo, S.; Ruderer, M. a.; Rawolle, M.; Körstgens, V.; Birkenstock, C.; Perlich, J.; Müller-Buschbaum, P. Evolution of Lateral Structures during the Functional Stack Build-up of P3HT:PCBM-Based Bulk Heterojunction Solar Cells. *ACS Appl. Mater. Interfaces* **2013**, *5*, 8581–8590.

(6) Park, H.; Howden, R. M.; Barr, M. C.; Bulović, V.; Gleason, K.; Kong, J. Organic Solar Cells with Graphene Electrodes and Vapor Printed poly(3,4-Ethylenedioxythiophene) as the Hole Transporting Layers. *ACS Nano* **2012**, *6*, 6370–6377.

(7) Gong, C.; Yang, H. B.; Song, Q. L.; Lu, Z. S.; Li, C. M. Mechanism for Dimethylformamide-Treatment of poly(3,4- Ethylenedioxythiophene): Poly(styrene Sulfonate) Layer to Enhance Short Circuit Current of Polymer Solar Cells. *Sol. Energy Mater. Sol. Cells* **2012**, *100*, 115–119.

DOI: 10.1021/acsami.5b02434
ACS Appl. Mater. Interfaces 2015, 7, 11069–11073

(8) Ouyang, J.; Chu, C. W.; Chen, F. C.; Xu, Q.; Yang, Y. High-Conductivity poly(3,4-Ethylenedioxythiophene):poly(styrene Sulfonate) Film and Its Application in Polymer Optoelectronic Devices. *Adv. Funct. Mater.* **2005**, *15*, 203−208.
(9) Yang, J. S.; Oh, S. H.; Kim, D. L.; Kim, S. J.; Kim, H. J. Hole Transport Enhancing Effects of Polar Solvents on poly(3,4-Ethylenedioxythiophene):poly(styrene Sulfonic Acid) for Organic Solar Cells. *ACS Appl. Mater. Interfaces* **2012**, *4*, 5394−5398.
(10) Xia, Y.; Ouyang, J. PEDOT:PSS Films with Significantly Enhanced Conductivities Induced by Preferential Solvation with Cosolvents and Their Application in Polymer Photovoltaic Cells. *J. Mater. Chem.* **2011**, *21*, 4927−4936.
(11) Mengistie, D. a; Ibrahem, M. a; Wang, P. C.; Chu, C. W. Highly Conductive PEDOT:PSS Treated with Formic Acid for ITO-Free Polymer Solar Cells. *ACS Appl. Mater. Interfaces* **2014**, *6*, 2292−2299.
(12) Kim, N.; Kee, S.; Lee, S. H.; Lee, B. H.; Kahng, Y. H.; Jo, Y. R.; Kim, B. J.; Lee, K. Highly Conductive PEDOT:PSS Nanofibrils Induced by Solution-Processed Crystallization. *Adv. Mater.* **2014**, *26*, 2268−2272.
(13) Zhou, J.; Lubineau, G. Improving Electrical Conductivity in Polycarbonate Nanocomposites Using Highly Conductive PEDOT/PSS Coated MWCNTs. *ACS Appl. Mater. Interfaces* **2013**, *5*, 6189−6200.
(14) Yeo, J. S.; Yun, J. M.; Kim, D. Y.; Park, S.; Kim, S. S.; Yoon, M. H.; Kim, T. W.; Na, S. I. Significant Vertical Phase Separation in Solvent-Vapor-Annealed poly(3,4-ethylenedioxythiophene):Poly-(styrene Sulfonate) Composite Films Leading to Better Conductivity and Work Function for High-Performance Indium Tin Oxide-Free Optoelectronics. *ACS Appl. Mater. Interfaces* **2012**, *4*, 2551−2560.
(15) Zhou, J.; Anjum, D. H.; Chen, L.; Xu, X.; Ventura, I. A.; Jiang, L.; Lubineau, G. The Temperature-Dependent Microstructure of PEDOT/PSS Films: Insights from Morphological, Mechanical and Electrical Analyses. *J. Mater. Chem. C* **2014**, *2*, 9903−9910.
(16) Xia, Y.; Sun, K.; Ouyang, J. Highly Conductive poly(3,4-Ethylenedioxythiophene):poly(styrene Sulfonate) Films Treated with an Amphiphilic Fluoro Compound as the Transparent Electrode of Polymer Solar Cells. *Energy Environ. Sci.* **2012**, *5*, 5325−5332.
(17) Zhang, W.; Zhao, B.; He, Z.; Zhao, X.; Wang, H.; Yang, S.; Wu, H.; Cao, Y. High-Efficiency ITO-Free Polymer Solar Cells Using Highly Conductive PEDOT:PSS/surfactant Bilayer Transparent Anodes. *Energy Environ. Sci.* **2013**, *6*, 1956−1964.
(18) Oh, J. Y.; Shin, M.; Lee, J. B.; Ahn, J. H.; Baik, H. K.; Jeong, U. Effect of PEDOT Nanofibril Networks on the Conductivity, Flexibility, and Coatability of PEDOT:PSS Films. *ACS Appl. Mater. Interfaces* **2014**, *6*, 6954−6961.
(19) Tung, V. C.; Kim, J.; Cote, L. J.; Huang, J. Sticky Interconnect for Solution-Processed Tandem Solar Cells. *J. Am. Chem. Soc.* **2011**, *133*, 9262−9265.
(20) Dehsari, H. S.; Shalamzari, E. K.; Gavgani, J. N.; Taromi, F. A.; Ghanbary, S. Efficient Preparation of Ultralarge Graphene Oxide Using a PEDOT:PSS/GO Composite Layer as Hole Transport Layer in Polymer-Based Optoelectronic Devices. *RSC Adv.* **2014**, *4*, 55067−55076.
(21) Yu, J. C.; Jang, J. I.; Lee, B. R.; Lee, G. W.; Han, J. T.; Song, M. H. Highly Efficient Polymer-Based Optoelectronic Devices Using PEDOT:PSS and a GO Composite Layer as a Hole Transport Layer. *ACS Appl. Mater. Interfaces* **2014**, *6*, 2067−2073.
(22) Lee, E.; Ryu, J.; Jang, J. Fabrication of Graphene Quantum Dots via Size-Selective Precipitation and Their Application in Upconversion-Based DSSCs. *Chem. Commun.* **2013**, *49*, 9995−9997.
(23) Lang, U.; Muller, E.; Naujoks, N.; Dual, J. Microscopical Investigations of PEDOT:PSS Thin Films. *Adv. Funct. Mater.* **2009**, *19*, 1215−1220.
(24) Zhou, J.; Li, E. Q.; Li, R.; Xu, X.; Ventura, I. A.; Moussawi, A.; Anjum, D. H.; Hedhili, M. N.; Smilgies, D.-M.; Lubineau, G.; Thoroddsen, S. T. Semi-Metallic, Strong and Stretchable Wet-Spun Conjugated Polymer Microfibers. *J. Mater. Chem. C* **2015**, *3*, 2528−2538.
(25) Kim, N.; Lee, B. H.; Choi, D.; Kim, G.; Kim, H.; Kim, J. R.; Lee, J.; Kahng, Y. H.; Lee, K. Role of Interchain Coupling in the Metallic State of Conducting Polymers. *Phys. Rev. Lett.* **2012**, *109*, 1−5.
(26) Alemu, D.; Wei, H.-Y.; Ho, K.-C.; Chu, C.-W. Highly Conductive PEDOT:PSS Electrode by Simple Film Treatment with Methanol for ITO-Free Polymer Solar Cells. *Energy Environ. Sci.* **2012**, *5*, 9662−9671.
(27) Hu, Z.; Zhang, J.; Zhu, Y. Effects of Solvent-Treated PEDOT:PSS on Organic Photovoltaic Devices. *Renewable Energy* **2014**, *62*, 100−105.

DOI: 10.1021/acsami.5b02434
ACS Appl. Mater. Interfaces 2015, 7, 11069−11073